ELSEVIER

New simple properties of a few irregular systems

B. Sapoval[a,b,*], J.S. Andrade Jr.[c], A. Baldassarri[d],
A. Desolneux[e], F. Devreux[a], M. Filoche[a,b],
D. Grebenkov[a], S. Russ[f]

[a]*Laboratoire de Physique de la Matière Condensée, C.N.R.S. Ecole Polytechnique, 91128 Palaiseau, France*
[b]*Centre de Mathématiques et de leurs Applications, Ecole Normale Supérieure, 94140 Cachan, France*
[c]*Departamento de Física, Universidade Federal do Ceará, 60451-970 Fortaleza, Ceará, Brazil*
[d]*INFM, UdR Roma 1, Dipartimento di Fisica, Università di Roma "La Sapienza", P.le Aldo Moro 2, 00185 Rome, Italy*
[e]*Laboratoire de Mathématiques Appliquées MAP5, Université Paris 5, 75006 Paris, France*
[f]*Institut für Theoretische Physik III, Universität Giessen, D-35392 Giessen, Germany*

Available online 20 June 2005

Abstract

This paper presents seven results on irregular systems that are both new and can be described simply. The first three results are related to dynamical and static properties of gradient percolation. Firstly, it is shown that the transient regimes which lead to self-organized gradient percolation due to corrosion do not scale like gradient percolation itself. Secondly, it is shown that there is no diffusion front in 1-D but there exists a zone of fluctuations with a size of the order of the system size. Thirdly, the geometry of realistic intermetallic contacts in 3-D is shown to be closely related to that of diffusion fronts, but different. The two next results are related to reactive irregular surfaces. Firstly, molecular dynamics results indicates that, in 2-D, the size of the active zone of purely absorptive surfaces in the Knudsen diffusion regime is larger than that found in the molecular diffusion regime. Secondly, it is then shown that, in this last regime, the particles that really interacts with the surface, remains near the surface within a distance equal to the unscreened perimeter length. The following topic is related to the vibrations of deterministic surface fractals: with very good approximation, the extended disordered modes can be described as a superposition of regular (non-localized) trivial modes of the initiator of the fractal morphology. Finally, it is shown that the diffusion reorganized

*Corresponding author. Laboratoire de Physique de la Matière Condensée, C.N.R.S. Ecole Polytechnique, 91128 Palaiseau, France. Tel.: +33 1 6933 4172; fax: +33 1 6933 3004.
E-mail address: bernard.sapoval@polytechnique.fr (B. Sapoval).

aggregation mechanism may display transitory fractal states with a life time increasing so rapidly with the system mass that dynamical equilibrium may never been reached, even for systems of relatively small size. This could be a simple example of the so-called "inherent states".

1. Transient versus final scaling in self-organized etching gradient percolation

Some 20 years ago, Michel Rosso, Jean-Francois Gouyet and Bernard Sapoval were interested in the geometrical features of a front of independently diffusing particles. This problem, inspired by the properties of diffused contacts, opened the way to the introduction of a general model, called the gradient percolation model or GP [1]. Introducing a spatial gradient in the occupation probability of the 2-D percolation model [2] naturally defines an irregular random interface, separating the infinite cluster in the region where $p \gg p_c$, from the under-critical region, where $p \ll p_c$. This so-called gradient percolation front spans the whole system (of width L_0), crossing the lattice in a direction transversal to the imposed gradient, in a region where $p \simeq p_c$ [3]. Careful studies showed that the fractal properties of the interface can be related to the fractal properties of the critical percolation cluster. Such facts were also observed in the final stages of dynamic collective invasion modeling corrosion or marine erosion, both phenomena that progressively build gradient percolation [4,5]. In a different and recent study it was found that GP fractal exponents can be used down to very small size. In other words, *non-fractal regimes exists, where it is possible to recognize the signature of criticality even in the absence of fractality* [6]. There exist then a specific type of criticality which exist even for very small systems, *in a limit opposite to the thermodynamic limit*. As extreme gradient fronts look very alike rough transitory fronts observed in etching the question arises of their exact similarity or not. As shown below they are different.

In 2-D, the GP front is described by its statistical width σ and its total length N_f. The only parameter governing these quantities is the applied gradient which, in the simplest case, spread uniformly on a distance L_g. The smaller the gradient, the wider the interface and the front width σ represents a good estimate of the geometrical correlation length. The interface is fractal up to a distance close to σ. As a consequence, the whole interface can be thought as a composed by L_0/σ independent fractal regions of linear size σ, each of them being a fractal set of dimension $D_f = \frac{7}{4}$, hence containing a number of points proportional to σ^{D_f}. The total number of point of an interface extended on a size L_0 (larger than σ) is thus proportional to

$$N_f \propto \sigma^{D_f}\left(\frac{L_0}{\sigma}\right) = L_0\sigma^{D_f-1} \ .$$

Surprisingly this scaling law between N_f and σ holds even for very large gradient, i.e., for very tiny *non-fractal* interfaces, for which σ is of order a few units [6].

We now consider the relation between length and width for the transitory interfaces generated by the dynamical process that leads from smooth interfaces to fractal critical GP geometries. Is it possible, even in this case, to characterize an irregular, but not yet fractal, interface produced transiently by the same exponents that characterizes fractal or extreme gradient interfaces? We will consider the specific case of the model of corrosion proposed in Ref. [4] to describe experiments of the etching of a 2-D aluminum films plunged in a finite volume of corrosive solution. This 2-D film is thought to be constituted by a collection of independent solid units presenting random resistance to etching. The etching power of the solution is supposed to be proportional to the etchant concentration: n/V, where n is the number of etching molecules and V the volume of the solution. When a solid unit come in contact with the liquid, two type of events can occur: 1/either its resistance is smaller than the etching power and the solid unit is dissolved and, consequently, the number of etchant molecules is decreased by 1 ($n(t+1) = n(t) - 1$) or 2/it has a resistance larger than the etching power and nothing happens. The diffusion of the etchant is supposed to be rapid enough so that the liquid remains always homogeneous. The phenomenology produced by this extremely simple model reproduces the main features observed in the experiment: the corrosion proceeds first with a constant velocity and a slightly irregular interface. Then the dynamics slows down, the interface fluctuates and becomes more and more irregular and finally the process stops spontaneously [4,7]. Furthermore, it has been shown that this dynamical process leads to Gradient Percolation universality class, with final fractal interface of dimension $\frac{7}{4}$ as the gradient percolation front [8]. The dynamics establishes spontaneously a spatial gradient of "corrosion" probability proportional to L_0/V. The surprise is that the same power laws are found to be observed in the case of very small volumes V that correspond to the extreme gradient case [9]. Even the non-fractal final interfaces obeys the same scaling law $N_f \propto \sigma^{D_f - 1}$ observed in the static (extreme) gradient percolation model. To sum up, whether rough interfaces arise from imposed static (and possibly large) gradients, or are created in the final GP etching, the power law relating the length and the width of the fronts are the same as that observed for the fractal fronts. In both cases the width and the length are implicit functions of the gradient, whatever its source.

The new computations presented here consider the relation between N_f and σ *during* the dynamical regime. In this case the interface is not fractal, but slightly irregular, and then more and more so. During the evolution, the width and the length are increasing functions of time. We have performed extended numerical simulations in order to measure the relation between length and width, but now with the time as the implicit variable. And what we find is very different from GP or extreme GP. This is shown in Fig. 1, where one observes that the now *transitory* relation is roughly: $N_f \propto \sigma$. This is in contrast with the gradient percolation scaling law which still holds for the final configuration of the interfaces as obtained *at the end of the very same simulations*. This is shown very clearly in the inset of Fig. 1. Note that the circles which represents the final states in Fig. 1 do not correspond to the widest and longest fronts. The maxima are indeed obtained at exact criticality near the end of the process, as discussed in Ref. [7].
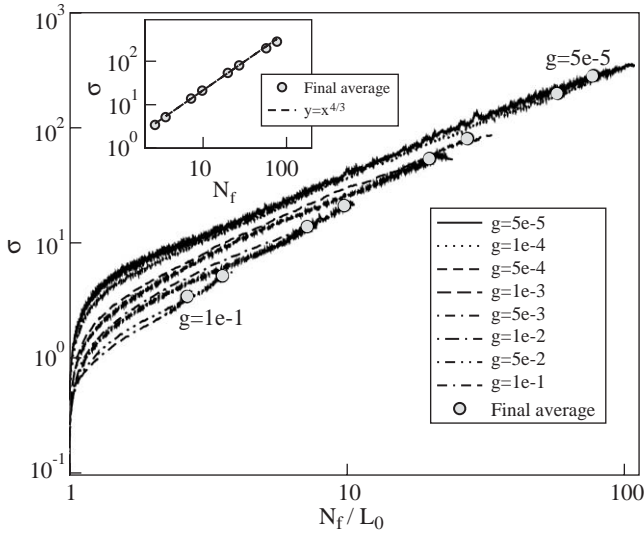
Fig. 1. Width σ of the liquid–solid interface versus its length during the corrosion dynamics. Here, time is a dummy variable. Each graph shows the results for 100 runs and its average for several values of the gradient $g = L_0/V$. The system size $L_0 = 2000$ for every value of g and the starting value of the probability is $p(0) = 1$. The circles indicates the final situations. The log–log scale shows a linear relation with an exponent equal to 1. In the inset the final averages are shown to scale according to the expected scaling relation (1) but here it is the gradient which is the dummy variable.

In conclusion, the relation between the length and the width of an irregular interface not necessarily fractal may in principle be a clue to decide whether its morphology is transitory or reflects some kind of final criticality linked to a self-organized gradient percolation scheme.

2. One-dimensional gradient percolation: A system which presents a zone of fluctuations with the size of the entire system

In gradient percolation [1], one introduces a spatial gradient in the occupation probability of particles on a lattice. In 2-D, this naturally defines the GP interface mentioned in the previous section. It brings the practical advantage that, in order to measure critical properties of percolation, no fine-tuning is necessary to adjust the critical parameter p to its non-universal threshold value p_c [3]. Up to now, no attention was given to the same problem in 1-D. This is what we discuss below.

The 1-D classical percolation (where all the sites are independent and occupied with probability p) is a well-known and trivial situation: the critical probability is $p_c = 1$ and the size distribution of clusters can be exactly computed. If one starts from a point, for example the origin 0, one can compute the mean distance d_c at which we first meet an empty site. The probability to find the first empty site at the

position k is $p^k(1-p)$, and thus

$$d_c = \sum_{k=0}^{\infty} k p^k (1-p) = \frac{p}{1-p} \ .$$

As the initial site is occupied the average cluster size is $1 + d_c = 1/(1-p)$.

The 1-D linear gradient percolation situation is the following: we have $L_g + 1$ sites (where L_g denotes the gradient length) which are all independent, and the site number k, with $0 \leqslant k \leqslant L_g$, is occupied with probability $p(k) = 1 - k/L_g$. This system is illustrated on Fig. 2. One can also in this case ask the question: starting from the origin 0 (which is always here an occupied site), where do we meet the first empty site? In other words, the question is: what is the size of the fluctuation zone Δ_f defined as the mean distance between the first empty site and the last occupied one. This length Δ_f can be exactly computed, in the following way: we first notice that thanks to the linear gradient, we have a symmetry between occupied and empty sites, and thus $\Delta_f = L_g - 2\mathbf{E}(T)$, where T is the position of the first empty site after the origin. We then can easily (thanks again to the linear gradient) compute

$$\mathbf{E}(T) = \sum_{k=1}^{L_g - 1} \mathbf{P}(T \geqslant k) = \sum_{k=1}^{L_g - 1} p(0)p(1)\ldots p(k)$$

$$= \sum_{k=1}^{L_g - 1} \frac{(L_g - 1)\ldots(L_g - k)}{L_g^k} = \frac{L_g!}{L_g^{L_g}} \sum_{k=0}^{L_g - 2} \frac{L_g^k}{k!} \ .$$

$$\simeq \frac{L_g!}{L_g^{L_g}} \times \frac{1}{2} e^{L_g} \simeq \sqrt{\frac{\pi L_g}{2}} \ .$$

This shows that when L_g is large, the first empty site is at a distance of the order $L_g^{1/2}$ and thus the size of the fluctuation zone is of the order of the gradient length L_g.
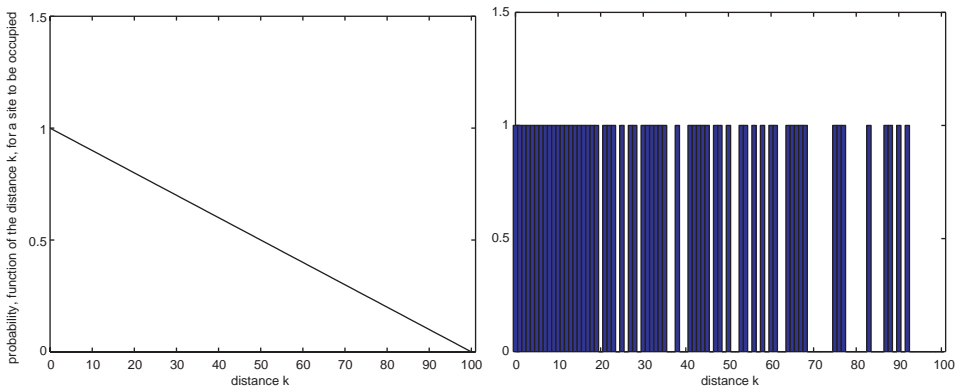

Fig. 2. 1-D linear gradient percolation. Left: probability for the site at distance k to be occupied, plotted as a function of k. It is linear, with a gradient length $L_g = 100$ on this figure. Right: example of a configuration $X_0, X_1, \ldots, X_{L_g}$ obtained with this gradient percolation situation, where $X_k = 1$ when the site k is occupied.

In that sense, the peculiarity of gradient percolation in 1-D is that the distance between the infinite occupied cluster (starting with $p = 1$) and the infinite empty cluster (finishing at $p = 0$) is of the order of the system size L_g whatever its value. In consequence, there is no gradient percolation front in 1-D.

3. The geometry of diffused intermetallic contacts

The 1-D gradient percolation discussed in the previous section could figure the situation of a 1-D intermetallic contact between A and B species with occupied sites representing A-atoms and empty sites representing B atoms. However, in the simplest quantum representation of interactions between single atomic orbitals, only first nearest neighbors (f.n.n.) share electrons. In that case the metallic A region would be separated from the metallic B region by the large fluctuation zone described above. It is generally considered that such a region would be insulating so that no electric conduction can cross this intermediate region.

In 2-D the only lattice where the A metallic region would be next to the B metallic region is the triangular lattice for which $p_c = \frac{1}{2}$ [2]. For instance in the square lattice with A f.n.n connections, the diffusion front represents the contact between A and B but with B connected by f.n.n. and second nearest neighbor (s.n.n.) connections. Due to the larger distance there would be only very weak hybridation between s.n.n. orbitals. In other words, in 2-D a direct A–B real electrical contact is only possible in the triangular lattice. In that case, the gradient percolation geometry would really represent the intermetallic contact geometry.

The situation is very different in 3-D where p_c is always smaller than $\frac{1}{2}$ [2]. Consequently, there is always a domain of concentration where both A and B systems are percolating. This makes it possible a true contact between the two regions. This is shown in Fig. 3 which displays a 2-D cross-section of the contact. The figure on the left shows the usual diffusion or GP front. In that case, the infinite cluster of the occupied A sites is constituted by the A-sites which are linked to $p = 1$ (bottom) through f.n.n. connections. However, the infinite cluster of the empty sites (B), which is built on the dual lattice, is made by B-sites which may be connected to $p = 0$ (top) either as f.n.n., or as s.n.n. or even as third-nearest neighbors (t.n.n.) [10]. But with the view of representing the electric contact between two metallic materials, this definition is artificial since the overlap between the orbitals of s.n.n. and t.n.n. is expected to be very small. The dark and light gray zones on the right shows the contact which is obtained when A and B play symmetric roles. The infinite clusters are made with f.n.n. connected sites for both A and B systems and the "contact" A-sites are the A-sites belonging to the A infinite cluster which are f.n.n. of a site of the B f.n.n. infinite cluster. The contact zone is obviously narrower than on the left since the definition of connections is more restrictive.

Fig. 4 displays the spatial variation of the probability for an A-site to belong either to the infinite cluster (a), to the diffusion front (b) or to the contact obtained when only f.n.n. interactions are allowed (c). One observes that in a large central region, the sites of the contact cluster (curve c) appear to belong to the diffusion front (b). It
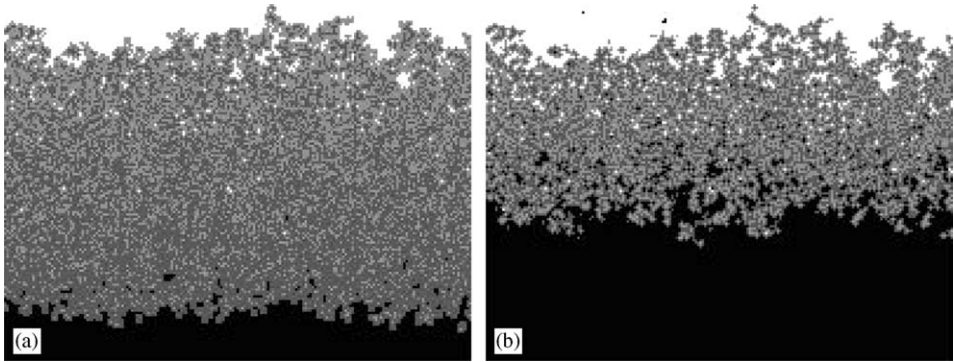
Fig. 3. A 2-D cross-section of the contact between A and B in the gradient percolation model in a cubic lattice with vertical $L_g = 200$. The A (resp., B) particles are shown in black or dark gray (resp., light gray or white). In (a) dark gray (A) and light gray (B) represents the usual diffusion front interface in a cubic lattice (see text). In (b), only the connections between first nearest neighbors (f.n.n.) are considered to represent the contact.
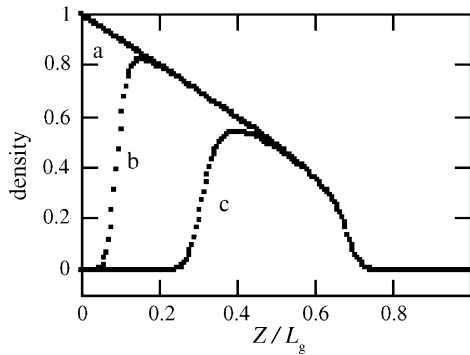

Fig. 4. Variation with z/L_g of the probability for an A-site to belong to the infinite cluster (a), to the diffusion front (b), or to the contact obtained when only f.n.n. AB contacts are considered (c). (z is the vertical direction on the previous figure). There exists a corresponding symmetric figure for the B sites pertaining to the contact.

follows that both the diffusion front and the contact have the same geometrical properties within their respective thickness. Then, the center part of the contact exhibit a fractal dimension equal to 3. In the narrow region where the concentration is close to the A percolation threshold, that is for z/L_g close to $1 - p_c = 0.683$ for a cubic lattice, the dimension is that of the incipient percolating cluster, close to 2.5 [2]. A symmetric situation exists for the B sites pertaining to the contact. Of course, in that situation the conducting properties of the A region would be certainly perturbed by the B impurities and reciprocally for the B region. This constitutes a new interesting but open question.

4. Diffusive transport towards irregular surfaces: Laplacian transport versus Knudsen diffusion

The role of the surface morphology on porous catalysts activity is of current interest [11,12]. This role is intimately related to the accessibility by diffusion of reagents to the active sites located along an irregular reactive surface. The concept of diffusive Laplacian fields includes the implicit assumption that molecular diffusion is the governing mechanism of mass transport. Such an approximation, however, can only be valid inside the void space between the protrusions of an irregular surface if the molecular mean free path is sufficiently smaller than the voids. Hence, Knudsen diffusion may become the dominant transport mechanism determining the system reactivity if the pressure is so low that the collisions among molecules are less frequent than collisions with the catalytic surface. The molecular mean free path therefore constitutes a lower cutoff for the validity of the molecular diffusion description.

In principle, the transition from molecular to Knudsen diffusion can only be predicted in terms of a microdynamical model. For this purpose, we adopt a Non-equilibrium Molecular Dynamics (NMD) Model method that has been originally proposed for the study of self-diffusion in pure fluids [13]. The technique is entirely based on the standard molecular dynamics (MD) at equilibrium, but includes a special scheme to identify and exchange *labeled* and *unlabeled* particles during the simulation. The details of this technique are presented elsewhere [14]. The diffusion cell used in these computations is a quadratic Koch curve with a diameter $L = 27$ and a total perimeter $L_p = 125$. A typical thermalized configuration of the system showing the positions of labeled particles is shown in Fig. 5.

Based on this NMD method, we have performed simulations for different densities corresponding to systems with $N = 1250$–$25\,000$ particles. From the solution, one can compute the local diffusive fluxes q_i crossing each element i of the interface. We measure the interface efficiency in terms of the active length L_a defined as

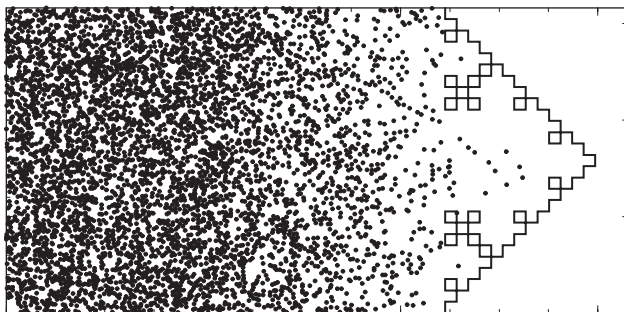$$L_a \equiv 1 / \sum_{i=1}^{L_p} \phi_i^2 \quad (1 \leqslant L_a \leqslant L_p), \tag{1}$$

Fig. 5. Typical configuration of the NMD system. Only the rough interface and the positions of labeled particles are shown.

where the sum is over the total number of interface elements L_p, and $\phi_i \equiv q_i / \sum q_j$ is the normalized mass flux at element i. From the definition (1), $L_a = L_p$ would indicate a limiting state of equal partition of fluxes ($\phi_i = 1/L_p$, $\forall i$).

As shown in Fig. 6, the computed active length decreases sharply with ρ down to a point where it remains constant at $L_a \approx 27$. These results are essentially independent of temperature. The decrease with density of the active length L_a reflects the transition from Knudsen to molecular diffusion. The mean free path Λ is inversely proportional to the particle density of the system, $\Lambda \propto 1/\rho$. For small ρ values, the mean free path of the particles is larger than the smaller length scale l of the irregular interface. At higher densities, the invariant behavior of L_a is a consequence of molecular diffusion and can be explained in terms of Makarov's theorem [15]. Precisely, the theorem states that *the information dimension of the harmonic measure on a singly connected interface in 2-D is exactly equal to 1*. In terms of activity, this means that, regardless the shape of the interface, the total length L_a of the region where most of the activity takes place should be of the order of the size or diameter L of the cell under a dilation transformation. Translating to our diffusion cell, where square Koch trees of third generation are the absorbing interfaces, the theorem of Makarov predicts that the value of L_a should be close to the size $L = 27$, in good agreement with the NMD limit obtained for denser systems.

One can also compute a value of the active zone length by direct numerical solution of the Laplace equation $\nabla^2 C = 0$ which represents the exact equation of the problem for molecules of very small sizes and high density. One obtains $L_a = 22.9$,
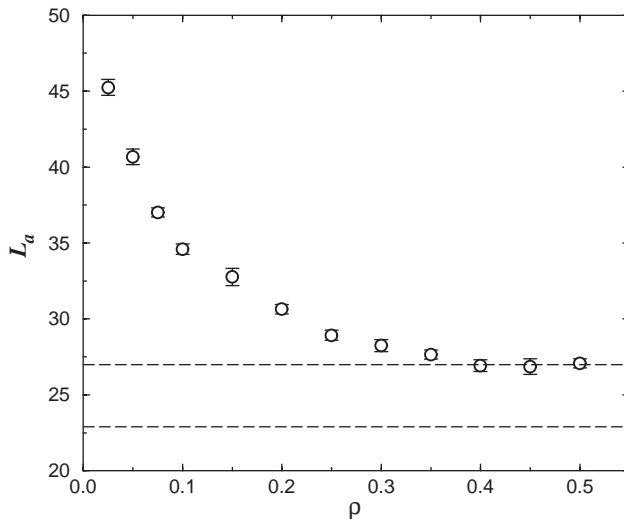

Fig. 6. Dependence of the active length L_a on the reduced density of the NMD cell. The average values with error bars refer to simulations with 5 different realizations of the NMD process. The horizontal dashed line at the top corresponds to the system size, $L_y = 27$. The one at the bottom indicates the value of the active length given from the simulation of the Laplacian fiend, $L_a = 22.9$.

also a value close to the size of the system $L = 27$. The origin of the small difference between the two values arises from the finite size of the particles used in the NMD computation. Note that the value of the active length that we find for small density is still smaller than L_p. This is due to the fact that, in this calculation, the surface is supposed to be perfectly absorbing. If even a very few reflections would be considered the entire perimeter would be working in the Knudsen regime but not in the Laplacian regime.

In summary, we have investigated through molecular dynamics the transition from Knudsen to molecular diffusion transport towards $2d$ absorbing interfaces with irregular geometry. Our results indicate that the length of the active zone decreases continuously with density from the Knudsen to the molecular diffusion regime. These observations may lead to new guidelines to the problem of diffusion and reaction on arbitrarily irregular interfaces.

5. The Brownian particles that are absorbed by a surface have travelled "along" this surface

This section also deals with the Laplacian transport that governs many transport processes in nature and industry. Examples can be found in electrochemistry, in physiology, and in heterogeneous catalysis [16]. In most real systems surfaces do not obey the Dirichlet boundary conditions considered above. Indeed, the global flux is governed by two transport phenomena, the volume transport to the surface characterized by the diffusivity and the transport across the surface measured by the permeability or the reactivity. In all cases, the ratio between surface and volume conductances introduces a physical length Λ characterizing a competition between these two effects [16]. The length Λ is also called the "unscreened perimeter length" as it measures the perimeter of a part of an irregular surface which works uniformly although being explored by Laplacian diffusing particles [17].

At a microscopic level, the surface permeability is proportional to the probability of absorption (or reaction) of diffusing particles colliding with the surface [18,19]. In other words, the particles have to hit the surface a number of times until being finally absorbed. A mathematical description of this stochastic motion leads to the so-called *partially reflected Brownian motion* (PRBM) characterized by the parameter Λ [20].

We address here the following question: *Before being absorbed, what is the size of the domain explored by the diffusing particles? Do they typically float near the boundary and at what distance?* This problem can be solved exactly for a flat surface. Firstly, let us consider the partially reflected Brownian motion on the upper half-space R_+^d $(d \geqslant 2)$ started from the origin. The probability density that this motion is finally absorbed in the vicinity ds of the boundary point $s = (s_1, \ldots, s_{d-1}, 0)$ has been calculated analytically in Ref. [20]:

$$t_\Lambda(s_1, \ldots, s_{d-1}) = \int_{-\infty}^{\infty} \ldots \int_{-\infty}^{\infty} \frac{dk_1 \ldots dk_{d-1}}{(2\pi)^{d-1}} \frac{e^{-i[k_1 s_1 + \cdots + k_{d-1} s_{d-1}]}}{1 + \Lambda |k|} \tag{2}$$

and due to rotational symmetry, this function depends only on the radius $r = (s_1^2 + \cdots + s_{d-1}^2)^{1/2}$. This probability density takes into account all possible Brownian trajectories from the origin to a vicinity of the boundary point s. The question we wish to answer here is to know what is the contribution of "flatten" trajectories near the boundary? For this purpose, one can introduce a *perfectly* absorbing barrier at some height h. The probability density that the PRBM started from the origin is finally absorbed in the vicinity of the boundary point s *without* touching the barrier at height h is found to be [20]:

$$t_\Lambda^{(h)}(s_1, \ldots, s_{d-1}) = \int_{-\infty}^{\infty} \cdots \int_{-\infty}^{\infty} \frac{dk_1 \ldots dk_{d-1}}{(2\pi)^{d-1}} \frac{e^{-i[k_1 s_1 + \cdots + k_{d-1} s_{d-1}]}}{1 + \Lambda |k| \coth(h|k|)} \ . \tag{3}$$

It is also rotationally invariant. The integration of the density $t_\Lambda^{(h)}(s_1, \ldots, s_{d-1})$ over the whole surface ∂R_+^d gives the probability that the PRBM is finally absorbed on the flat boundary *without* touching the barrier at height h:

$$\int_{-\infty}^{\infty} \cdots \int_{-\infty}^{\infty} ds_1 \ldots ds_{d-1} t_\Lambda^{(h)}(s_1, \ldots, s_{d-1}) = \frac{1}{1 + \Lambda/h} \ .$$

This is the exact proportion of random trajectories (including the many collisions with the surface) which are finally absorbed without reaching the height h. Consequently, the length Λ provides the width of the layer near the boundary where a half of the diffusing particles exercise their motion (until absorption). For small values of Λ, only a small layer is explored.

In the same time, the length Λ determines the typical size of the region of the surface itself where half of diffusing particles are absorbed. Indeed, the relation (2) allows to calculate the probability $P_\Lambda(r)$ that the PRBM is finally absorbed on a disk of radius r around the origin. In two dimensions, this probability is found to be

$$P_\Lambda(r) = 1 - \frac{2}{\pi} \left(\frac{r}{\Lambda} \right) \int_0^{\infty} \frac{e^{-t} \, dt}{t^2 + (r/\Lambda)^2} \ .$$

In particular, one finds $P_\Lambda(\Lambda/2) \simeq 0.4522$, i.e., approximately half of the diffusing particles are absorbed on an interval $(-\Lambda/2, \Lambda/2)$ around the origin. For the 3-D case, one obtains

$$P_\Lambda(r) = 1 - \int_0^{\infty} \frac{t e^{-t} \, dt}{\sqrt{t^2 + (r/\Lambda)^2}}$$

and $P_\Lambda(\Lambda) \simeq 0.4611$. As a consequence, around half of the diffusing particles are absorbed on the disk of radius Λ.

The above results are exact for flat surfaces. In that case the "unscreened perimeter length" Λ determines approximately the volume near the surface where the absorption takes place. But the very significance of such results is that the same conclusions are valid for irregular surfaces. This can be justified by numerical studies of the PRBM near irregular boundaries. For instance, we have shown for Koch type boundaries that the second result is still valid, i.e. Λ represents an average perimeter of the characteristic absorption region of an irregular boundary [17,19]. This lead to

a practical suggestion in order to increase the efficiency of irregular interfaces as Laplacian exchangers. The idea is to use a diffusion source with a geometry following the Minkovski half-sausage at a distance of order Λ from the real surface. In such a situation the losses due to the access impedance will be minimized.

6. Disordered wave functions in deterministic fractal drums

The eigenfunctions $\psi(x,y)$ of deterministic fractal drums are studied numerically at high energies. Apart from some localized states, two characteristic types of eigenmodes exist, where the amplitudes either form a regular pattern or a disordered pattern. We show that both types of modes can be approximated by a special superposition of the eigenfunctions $\Phi_{n,m}(x,y)$ of the regular square initiator. Whereas a regular state of the fractal drum refers to one special pair of (n,m)-values, the disordered modes are superposition from those $\Phi_{n,m}(x,y)$ that have energies close to the energy of $\psi(x,y)$.

Fractal drums [21] represent a prominent example of irregular resonators. Deterministic fractal drums are constructed by fractal generators and the effect of the rough boundaries on their spectra and their eigenfunctions has been subject to intense research (see Ref. [22] and references therein). Here, we are interested in the shape of the eigenfunctions $\psi(x,y)$, which influence e.g. the behavior of the viscous damping. It is well-known that both, localized and extended modes exist and that the majority of the higher-energies modes is extended.

This work focuses on the extended modes, which can be either of regular or of disordered shape. Examples are shown in Fig. 7. The amplitudes of (a) look regular and can be interpreted as an eigenfunction of a square membrane of length L, $\Phi_{n,m}(x,y) = (2/L)\sin(n\pi x/L)\sin(m\pi y/L)$ with energy $E_{nm} = (\pi^2 c^2/L^2)(n^2 + m^2)$ and sound velocity c [21]. Both, $\phi_{n,m}(x,y)$ and $E_{n,m}$ refer to $(n,m) = (16, 16)$. The shape of mode (b), on the other hand, looks disordered and the distribution $P(\psi)$ (not shown here) is very close to a Gaussian distribution. This is typical for wave functions in irregular systems that are a random superposition of plane waves (see e.g. Ref. [23] and references therein).

In order to analyze the shape of the disordered modes, we expand them by the eigenfunctions $\Phi_{n,m}(x,y)$ of the square initiator. The coefficients are given by $C_{n,m}^{(\alpha)} = \int dx\, dy\, \Phi_{n,m}(x,y)\,\psi^{(\alpha)}(x,y)$, where $\psi^{(\alpha)}(x,y)$ is the αth wave function of the fractal drum and the integral is carried out over the area of the drum. The space, where the eigenfunctions form a complete basis (the square) differs from the one considered here. Nevertheless, we tested numerically that $\sum_{n,m}(C_{n,m}^{(\alpha)})^2 \approx 1$ for large α, which means that the modes of higher energies can be reasonably well described as superpositions from the eigenfunctions of the square. The results are presented in Fig. 8. The figure shows that the $C_{n,m}$ show large values only along a circle of radius $\sqrt{n^2 + m^2} \sim \sqrt{E^{(\alpha)}}$, where $E^{(\alpha)}$ is the energy of the mode $\psi^{(\alpha)}(x,y)$. This interesting behavior shows that only those $\Phi_{n,m}(x,y)$ contribute to $\psi^{(\alpha)}(x,y)$ that possess an

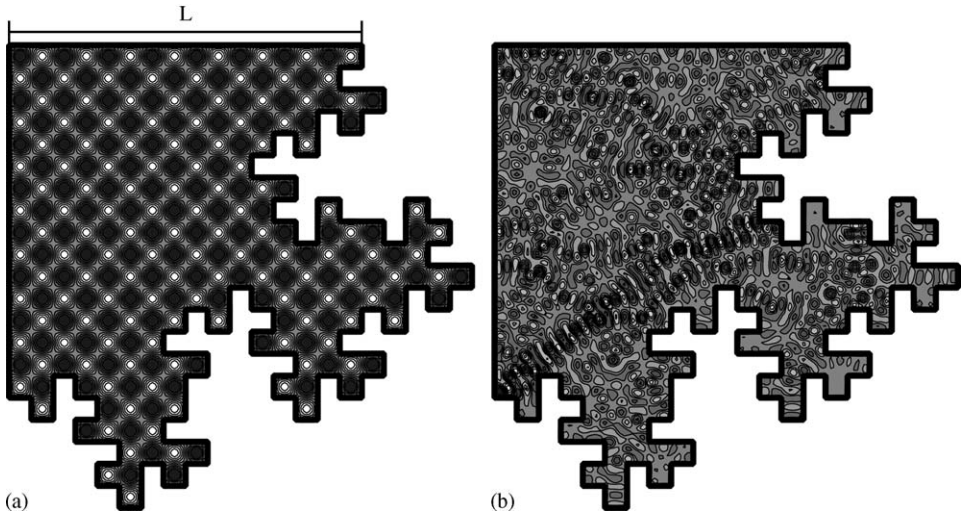Fig. 7. Two typical examples of non-localized eigenmodes under Dirichlet boundary conditions in fractal drums of unit side length L, where the fractal generator has been applied to two sides of a square system: (a) a regular "trivial" mode that corresponds to the mode $\Phi_{16,16}$ of a square membrane and (b) a disordered mode.
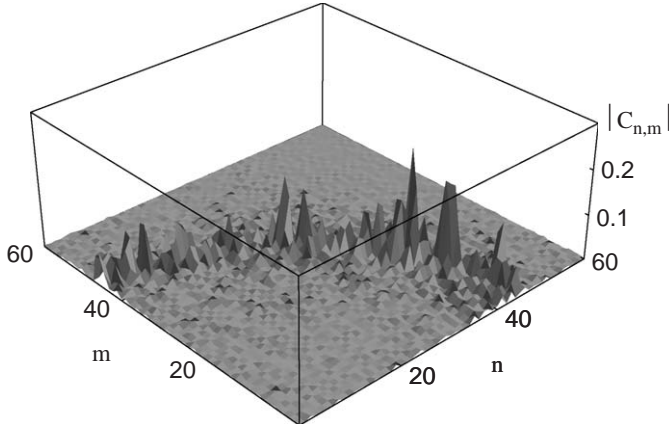

Fig. 8. The coefficients $C_{n,m}$ of the eigenmode of Fig. 1(b) in the basis of the eigenmodes $\Phi_{n,m}$ of the regular square system are shown. Note that this is really a decomposition in the reciprocal space of the square initiator.

energy $E_{n,m} \approx E^{(\alpha)}$. Similar to perturbation theory, the regular modes still play a role for the disordered modes and the ones with appropriate energy values are filtered to form the new disordered modes by superposition.

In summary, we have shown that the disordered extended modes of fractal drums can be described as a superposition of regular modes with energies from a narrow energy interval. Apparently, those modes form a stable disordered mode amplitude by random interference. Additionally to the typical example shown in this paper, we investigated many extended eigenmodes of higher energies, which all showed a similar behavior. The well-known "trivial" modes, on the other hand, can be described as one single regular mode of identical energy that fits exactly into the rough boundary features and possesses only one non-vanishing coefficient $C_{n,m}$.

7. Diffusion reorganized aggregates: A transient and fractal equilibrium

Diffusion Reorganized Aggregation (DRA) is a model that has been proposed by Filoche and Sapoval in 1999 [24,25]. It consists in an iterative process that progressively transforms a structure made of particles (or pixels). The DRA process is a surface to surface evaporation–diffusion–condensation process which conserves the total mass of the system. Its evolution mechanism proceeds in the following steps (Fig. 9):

(1) A particle is chosen at random on the surface of an initial structure and is dissolved, occupying an empty site next to its initial position.
(2) The dissolved particle may jump back to its original site or start a Brownian random walk on a square lattice which represents the outer medium. The time step for each jump is $\tau = 1$. This motion is stopped when the particle hits the structure again as it sticks on first hit.
(3) The process, which conserves the total mass, is then iterated. For practical reasons, the system is enclosed in a large square window: whenever a diffusing particle strikes the window, this particle is reinitiated on another site of this external box, following a probability law that simulates the random walk in the infinite outer medium. As the probability to return to a starting site is equal to 1 in $d = 2$, this does not modify the morphologies which are generated by the process. The existence of the external box only perturbs the time scale so that the
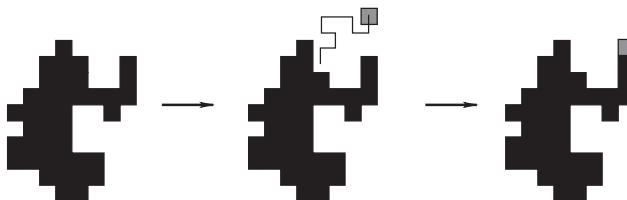

Fig. 9. Elementary evaporation–diffusion–condensation mechanism. The structure evolves by iterating this process.

number of computer steps is not proportional to a real time. For this reason, the number of steps is called pseudo-time.

The DRA process differs from the DLA process [26], as here particles are not launched from infinity but from the surface of the cluster itself. It is then a mass conserving process, very different from DLA growth.

Starting from any compact structure, for example a disk, the DRA process rapidly creates several branches. After a long relaxation period, the system reaches a dynamical fractal structure (Fig. 10). Furthermore, the geometrical features are found to be identical when starting from other initial structures such as a DLA tree. The DRA structure appears as a final equilibrium state towards which any initial morphology of M particles will converge after sufficient number of DRA iterations. It can then be considered as a general statistical attractor for that specific dynamical process.

The properties of the DRA structure are the following: firstly, this structure is statistically isotropic. Secondly, a mass versus radius plot of the final structure shows that it is fractal with a fractal dimension $D_f \approx 1.75 \pm 0.02$ in two dimensions. Thirdly, unlike the DLA structure, also obtained through a diffusion–aggregation process, the DRA structure has very small spatial and time correlations.

However, in 2002, it has been shown by Großkinsky et al. that any process that is a Markov chain with an evolution mechanism satisfying a detailed balance condition, will after a very long time, converge to a structure pertaining to the universality class of the lattice animals [27]. These lattice animals differ from the DRA structures on two important features: first, their fractal dimension is $D \approx 1.56$ in two dimensions, second they have an anisotropic shape, even though the model is purely isotropic [28]. And simulations ran on *small* initial clusters, for instance a disk of a few hundreds particles, confirm that the end structure is not isotropic and that
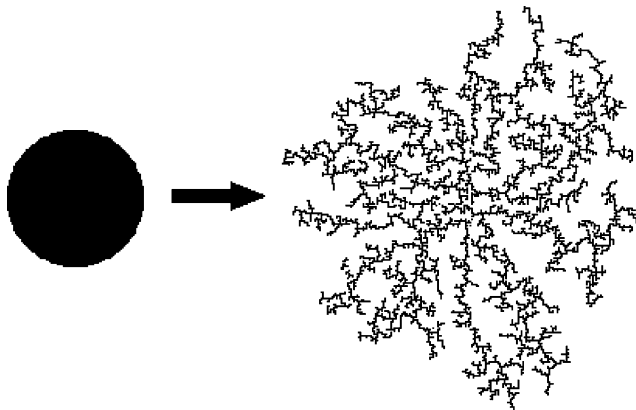

Fig. 10. Example of the dynamical structure obtained after 2 billion timesteps when starting from a disk made of 8000 particles. The final structure is branched, statistically isotropic and has a fractal dimension $D_f \approx 1.75$.

the "fractal dimension" that can be measured is around 1.6. Nevertheless, for a cluster of 8000 particles, numerical simulations have shown that, once reached, the DRA structure remains stable for more than 1 billion timesteps (the time unit being the jump rate on the lattice) and that no transition towards the lattice animal structure is observed. So, we are left with an apparent contradiction: why do we observe that the DRA remains unchanged, even after a very long simulation time, although it does not correspond to the theoretical dynamical equilibrium?

Our hypothesis is that the DRA structure is only a transient state but whose duration is expected to diverge rapidly with the cluster size. In that sense, it would belong to the so-called *inherent states* of the system, as introduced by Edwards [29]. Further simulations have to be carried out to confirm this idea. Such behavior is typical of a non-ergodic system. In fact, it seems to be as if the DRA process would not allow a rapid enough exploration of the entire configuration space and would "freeze" the system into a "transient equilibrium" (the DRA structure), hence the origin of the non-ergodicity.

In summary, simply putting the source on the structure itself and not at infinite distance (as in the case of the DLA) drastically modifies the characteristics of the diffusion and aggregation dynamics. In all cases, the DRA process leads to an isotropic fractal structure of fractal dimension around 1.75. The dynamical properties of this structure (duration, ergodicity) still remain open questions that have to be investigated, both by numerical simulations and theoretical analysis.

References

[1] B. Sapoval, M. Rosso, J.F. Gouyet, The fractal nature of a diffusion front and relation to percolation, J. Phys. Lett. (Paris) 46 (1985) L149.
[2] D. Stauffer, A. Aharony, Introduction to Percolation Theory, second ed., Taylor & Francis, London, 1994.
[3] M. Rosso, J.F. Gouyet, B. Sapoval, Determination of percolation probability from the use of a concentration gradient, Phys. Rev. B 32 (1985) 60533.
[4] B. Sapoval, S.B. Santra, P. Barboux, Stable fractal interfaces in the etching of random systems, Europhys. Lett. 41 (1998) 297.
[5] B. Sapoval, A. Baldassarri, A. Gabrielli, Self-stabilized fractality of Sea-coasts through erosion, Phys. Rev. Lett. 99 (2004) 098501-1.
[6] A. Desolneux, B. Sapoval, Percolation fractal exponents without fractals, see cond-mat/0210106, submitted for publication.
[7] S.B. Santra, B. Sapoval, Critical fluctuations and self-organized fractality in chemical reactions: spontaneous gradient percolation in the etching of random solids, Physica A 266 (1999) 160.

 [8] A. Gabrielli, A. Baldassarri, B. Sapoval, Surface hardening and self-organized fractality through etching of random solids, Phys. Rev. E 62 (2000) 3913.
 [9] A. Desolneux, B. Sapoval, A. Baldassarri, Self-organised percolation power laws with and without fractal geometry in the etching of random solids, in: M.L. Lapidus, M. van Frankenhuijsen (Eds.), Fractal Geometry and Applications: A Jubilee of Benoit Mandelbrot, Proceedings of the Symposia on Pure Mathematics, vol. 72 (Part 2), 2004, pp. 485–505, pre-print `cond-mat/0302072`
[10] J.-F. Gouyet, M. Rosso, B. Sapoval, Fractal structure of diffusion and invasion fronts in 3-D lattices through gradient percolation approach, Phys. Rev. B 37 (1988) 1832.
[11] M.-O. Coppens, The effect of fractal surface roughness on diffusion and reaction in porous catalysts—from fundamentals to practical applications, Catal. Today 53 (1999) 225.
[12] M. Sheintuch, Reaction engineering principles of processes catalyzed by fractal solids, Catal. Rev. 43 (2001) 233.
[13] J.J. Erpenbeck, W.W. Wood, in: B.J. Berne (Ed.), Statistical Mechanics, Part B: Time-dependent Processes, Modern Theoretical Chemistry, vol. 6, Plenum, New York, 1977.
[14] J.S. Andrade Jr., H.F. da Silva, M. Baquil, B. Sapoval, Phys. Rev. E 68 (2003) 041608.
[15] N.G. Makarov, On the distortion of boundary sets under conformal mapping, Proceedings of the London Mathematical Society, vol. 51, 1985, p. 369; P. Jones, T. Wolff, Hausdorff dimension of harmonic measure in the plane, Acta Math. 161 (1988) 131.
[16] B. Sapoval, Transport across irregular interfaces: fractal electrodes, in: A. Bunde, S. Havlin (Eds.), Fractals and Disordered Systems, Springer, Berlin, 1996, p. 233.
[17] B. Sapoval, General formulation of Laplacian transfer across irregular surfaces, Phys. Rev. Lett. 73 (1994) 3314.
[18] M. Filoche, B. Sapoval, Can one hear the shape of an electrode, II: theoretical study of the Laplacian transfer, Eur. Phys. J. B 9 (1999) 755.
[19] D.S. Grebenkov, M. Filoche, B. Sapoval, Spectral properties of the Brownian self-transport operator, Eur. Phys. J. B 36 (2003) 221.
[20] D.S. Grebenkov, Laplacian Transport towards Irregular Interfaces: A, Theoretical, Numerical and Experimental Study, Ph.D. Thesis, Ecole Polytechnique, France; Partially reflected Brownian motion: a stochastic approach to transport phenomena, in: Focus on Probability Theory, vol. 1, Nova Publisher, New York, 2004, to appear.
[21] B. Sapoval, T. Gobron, Vibrations of strongly irregular or fractal resonators, Phys. Rev. E 47 (1993) 3013.
[22] S. Russ, J. Mellenthin, Periodic orbit theory in fractal drums, J. Phys. A, 2005, this volume.
[23] Y. Hlushchuk, S. Russ, Level statistics and eigenfunctions of pseudointegrable systems: dependence on energy and genus number, Phys. Rev. E 68 (2003) 016203.
[24] M. Filoche, B. Sapoval, Dynamical fractal equilibrium in diffusion limited reorganization, C. R. Acad. Sci. Paris Série II b 327 (1999) 1071.
[25] M. Filoche, B. Sapoval, Diffusion-limited reorganization: attractors in diffusion process?, Phys. Rev. Lett. 85 (2000) 5118.
[26] T.A. Witten, . Jr, L.M. Sander, Diffusion-limited aggregation, a kinetic critical phenomenon, Phys. Rev. Lett. 47 (1981) 1400–1403.
[27] S. Großkinsky, M. Timme, B. Naundorf, Universal attractors of reversible aggregate-reorganization processes, Phys. Rev. Lett. 88 (2002) 034501.
[28] F. Family, T. Vicsek, P. Meakin, Are random fractal clusters isotropic?, Phys. Rev. Lett. 55 (1985) 641.
[29] S.F. Edwards, R.B.S. Oakeshott, Physica A 157 (1989) 1080;
     A. Mehta, S.F. Edwards, Physica A 157 (1989) 1091.